

LABORATÓRIO DE INSTRUMENTAÇÃO E
FÍSICA EXPERIMENTAL DE PARTÍCULAS

LIP / 98-02

September 1998



EXT-2000-071

16/10/1998

RESULTS ON CHARMONIUM STATES IN Pb-Pb INTERACTIONS

Sérgio Ramos^{1?)}

LIP-Lisbon

and

IST, Universidade Técnica de Lisboa

NA50 Collaboration

Abstract

We present cross-sections for J/ψ , ψ' and Drell-Yan production in lead-lead interactions at 158 GeV/nucleon. The Pb-Pb data, when compared with previous results obtained with lighter target or projectiles, show a similar behaviour for Drell-Yan, but exhibit an anomalous J/ψ suppression, which increases with centrality.

Talk presented at XXIX International Conference on High Energy Physics
Vancouver, Canada, July 1998

¹LIP, Av. Elias Garcia 14, P-1000 Lisboa, Portugal (e-mail: siocha@lip.pt)

RESULTS ON CHARMONIUM STATES IN Pb-Pb INTERACTIONS

Presented by SÉRGIO RAMOS, *LIP-Lisbon*

NA50 COLLABORATION

C. BAGLIN, A. BUSSIÈRE, V. CAPONY

LAPP, CNRS-IN2P3, Annecy-le-Vieux, France

A. BALDIT, J. CASTOR, T. CHAMBON, I. CHEVROT, A. DEVAUX, B. ESPAGNON,

J. FARGEIX, P. FORCE, S. MOURGUES, P. SATURNINI
LPC, Univ. Blaise Pascal and CNRS-IN2P3, Aubière, France

C. ALEXA, V. BOLDEA, S. CONSTANTINESCU, S. DITA

IFA, Bucharest, Romania

C. CICALÒ, A. DE FALCO, P. MACCIOTTA, A. MASONI, G. PUDDU, S. SERCI,

P. TEMNIKOV, G.L. USAI

Università di Cagliari/INFN, Cagliari, Italy

C. LOURENÇO, E. SCOMPARIN^g, P. SONDEREGGER^b

CERN, Geneva, Switzerland

M.C. ABREU^a, P. BORDALO^b, L. CASAGRANDE, J. CRUZ,

C. QUINTANS, S. RAMOS^b, R. SHAHOYAN^h, S. SILVA, C. VALE

LIP, Lisbon, Portugal

S.N. FILIPPOV, Y.K. GAVRILOV, M.B. GOLUBEVA, F.F. GUBER,

T.L. KARAVITCHEVA, A.B. KUREPIN, N.S. TOPILSKAYA

INR, Moscow, Russia

J. ASTRUC, M.P. COMETS, C. GERSCHEL, D. JOUAN, Y. LE BORNEC,

M. MAC CORMICK, X. TARRAGO, N. WILLIS

IPN, Univ. de Paris-Sud and CNRS-IN2P3, Orsay, France

B. CHAURAND, F. FLEURET, M. GONIN, L. KLUBERG, P. PETIAU, A. ROMANA

LPNHE, Ecole Polytechnique and CNRS-IN2P3, Palaiseau, France

C. RACCA

IReS, Univ. Louis Pasteur and CNRS-IN2P3, Strasbourg, France

B. ALESSANDRO, R. ARNALDI, S. BEOLÈ, E. CHIAVASSA, N. DE MARCO,

G. DELLACASA^c, M. GALLIO, P. GIUBELLINO, M. IDZIK^d, A. MARZARI-CHIESA,

M. MASERA, A. MUSSO, A. PICCOTTI, W.L. PRADO DA SILVA^f, L. RAMELLO^c,

P. RATO-MENDES, L. RICCATI, S. SARTORI, C. SOAVE, E. VERCELLIN

Università di Torino/INFN, Torino, Italy

M. BEDJIDIAN, F. BELLAICHE, B. CHEYNIS, O. DRAPIER, J.Y. GROSSIORD,

A. GUICHARD, R. HAROUTUNIAN, F. OHLSSON-MALEK^e, J.R. PIZZI

IPN, Univ. Claude Bernard and CNRS-IN2P3, Villeurbanne, France

M. ATAYAN, A.A. GRIGORIAN, H. GULKANYAN, R. HAKOBYAN, S. MEHRABYAN

YerPhI, Yerevan, Armenia

a) also at FCUL, Universidade de Lisboa, Lisbon, Portugal

b) also at IST, Universidade Técnica de Lisboa, Lisbon, Portugal

c) Dipartimento di Scienze e Tecnologie Avanzate, II Facoltà di Scienze, Alessandria, Italy

d) now at Faculty of Physics and Nuclear Techniques, University of Mining and Metallurgy, Cracow, Poland

e) now at ISN, Univ. Joseph Fourier and CNRS-IN2P3, Grenoble, France

f) now at UERJ, Rio de Janeiro, Brazil

g) on leave of absence from Università di Torino/INFN, Torino, Italy

h) on leave of absence from YerPhI, Yerevan, Armenia

We present cross-sections for J/ψ , ψ' and Drell-Yan production in lead-lead interactions at 158 GeV/nucleon. The Pb-Pb data, when compared with previous results obtained with lighter target or projectiles, show a similar behaviour for Drell-Yan, but exhibit an anomalous J/ψ suppression, which increases with centrality.

1 Introduction

NA50 is a CERN fixed target experiment designed for the study of Pb-Pb collisions in the North Area High Intensity Facility of the SPS accelerator. It is the upgrade of the previous NA38 experiment which took data from 1986 to 1992, using proton, oxygen and sulphur beams.

NA50 is devoted to the detection of the Quark-Gluon Plasma (QGP) formation. It studies charmonium production, considered as an unambiguous signature¹.

2 Experimental setup

The NA50 detector² consists mainly of a muon spectrometer, an active target formed by several lead subtargets, an electromagnetic calorimeter, a forward hadronic calorimeter and a charged multiplicity detector.

The muon spectrometer is based on eight multi-wire proportional chambers and a toroidal air-gap magnet. It covers the pseudo-rapidity interval $2.8 < \eta_{lab} < 4.0$. Four highly segmented scintillator hodoscopes perform the dimuon trigger, whereas two other are used for trigger efficiency measurements. The hadron absorber, located between the target region and the muon spectrometer, consists of a 60 cm long BeO preabsorber, followed by 400 cm of carbon and 80 cm of iron. An iron wall at the end of the spectrometer, before the last trigger hodoscope, ensures that the triggering particles are indeed muons.

The active target assembly is formed by a set of seven individual lead subtargets, 1 or 2 mm thick, with total interaction length L_{int} , as shown in Table 1. Each subtarget is followed by pairs of quartz blades, located on the left and the right of the beam axis, used to identify the vertex interaction and fight spectator fragment reinteractions. Two anti-halo quartz counters, located immediately upstream from the subtargets, sign preinteractions.

A beam hodoscope (BH), subdivided in sixteen quartz counters, located 22 m upstream from the target, is used to count the incoming lead ions and to reject beam pile-up. It is followed downstream by an interaction detector (BHI) which tags interactions in the BH itself.

The electromagnetic calorimeter, located 32 cm downstream from the target centre, surrounds the BeO preabsorber, and thus covers a pseudo-rapidity interval outside the muon spectrometer acceptance: $1.1 < \eta_{lab} < 2.3$. It is subdivided in four rings and six sextants of roughly equal pseudo-rapidity ranges and

Table 1: Characteristics of the data samples

Period	L_{int}	Intensity	Nb. triggers	Nb. J/ψ
1996	30%	$5.4 \cdot 10^7$	$168 \cdot 10^6$	$275 \cdot 10^3$
1995	17.5%	$3.2 \cdot 10^7$	$58 \cdot 10^6$	$48 \cdot 10^3$

is made of scintillating optical fibres embedded in lead converter in a 1:2 volume ratio ($\langle L_{rad} \rangle = 0.93$ cm). Its resolution is 5% for central collisions. The neutral transverse energy, E_T , is obtained by subtracting the charged particle contribution, which is estimated (by Monte-Carlo) to amount to 40%.

The zero degree calorimeter is a very forward detector ($\eta_{lab} \geq 6.2$) measuring the energy of the beam spectator fragments, E_{ZDC} (by means of the Čerenkov light produced in the fibres). It is located 165 cm downstream from the target centre, near the beam axis, protected against secondaries produced in the interaction by a long conical Cu collimator. It is made of SiO₂ optical fibres embedded in a tantalum converter in a 1:17 volume ratio. Its resolution is 7% for 32.7 TeV incident ²⁰⁸Pb nuclei.

The multiplicity detector is a two plane highly segmented silicon microstrip device, measuring charged particle multiplicities within the pseudo-rapidity range $1.5 < \eta_{lab} < 3.5$. It has not been used in the present analysis.

3 Data analysis

Data have been collected with two different Pb target configurations, in 1995 and 1996, with a lead beam of 158 GeV/nucleon incident momentum. Details of the two data samples are given in Table 1.

The event selection criteria are as follows: the BH detects only one incident ion; no preinteraction is detected by the BHI or the halo counters; only two tracks are reconstructed in the fiducial region of the spectrometer; each image track, conceptually obtained from the real track by reversing the magnetic field, is also accepted by the apparatus so that muon acceptance is charge independent; interaction in one of the subtargets and no reinteraction, as assigned by the active target algorithm (in 1995); and, because of the target algorithm low efficiency for peripheral collisions use, for this type of events, of a contour cut based on a 2σ correlation between E_T and E_{ZDC} reinforced with a strong cut on the distance between each muon track and the beam axis (in 1996).

The purpose of this analysis is to study the dimuon yield in our high mass region, which originates from the J/ψ and ψ' decays as well as from the Drell-Yan mechanism.

The kinematical domain used is defined by: $2.92 \leq y_{lab} \leq 3.92$ (i.e., $0 \leq y_{cms} \leq 1$) and $|\cos \theta_{CS}| < 0.5$, leading, in the mass region of interest, to acceptances of the order of 15%. The J/ψ mass resolution is 96 MeV (3.1%) and increases to 104 MeV (3.3%) for the most peripheral events recovered by the $E_T - E_{ZDC}$ contour cut.

In this analysis the background and the open charm ($D\bar{D}$) contributions are also taken into account. The background is mainly due to uncorrelated π and K decays into muons. It is computed from the like-sign mass distributions dN/dM^{++} and dN/dM^{--} using the relation

$$\frac{dN^{Bg}}{dM} = 2R \cdot \left[\sqrt{\left(\frac{dN^{++}}{dM} \cdot \frac{dN^{--}}{dM} \right)_{field+}} + \sqrt{\left(\frac{dN^{++}}{dM} \cdot \frac{dN^{--}}{dM} \right)_{field-}} \right],$$

where R is a factor depending on the type of the collision. For ion induced reactions, $R = 1$.

The opposite sign muon pair invariant mass distribution is fitted according to the following procedure in order to determine the amounts of its different components. The shapes of the muon pairs originating from the J/ψ and ψ' decays and from the Drell-Yan mechanism are obtained from a simulation of the NA50 detector using the same reconstruction and selection criteria as used for the real data. Drell-Yan contribution is calculated at the leading order and uses the MRS43 structure functions³, which take into account the \bar{u}/\bar{d} asymmetry as measured by NA51 experiment⁴. The $D\bar{D}$ shape is taken from Pythia and its amplitude is previously fixed by fitting the data in the range $1.9 < M_{\mu\mu} < 2.9$ GeV/ c^2 , allowing for a charm-like excess⁵. Finally, the amplitudes of J/ψ , ψ' and Drell-Yan contributions are obtained from a fit to the experimental data (above $M_{\mu\mu} > 3.05$ GeV/ c^2), according to:

$$\frac{dN^{+-}}{dM} = A_{J/\psi} \cdot \frac{dN^{J/\psi}}{dM} + A_{\psi'} \cdot \frac{dN^{\psi'}}{dM} + A_{DY} \cdot \frac{dN^{DY}}{dM} + \frac{dN^{D\bar{D}}}{dM} + \frac{dN^{Bg}}{dM},$$

with five free parameters: $A_{J/\psi}$, $A_{\psi'}$, A_{DY} , $M_{J/\psi}$ and $\sigma_{J/\psi}$; the ψ' mass and width are functions of the corresponding J/ψ values.

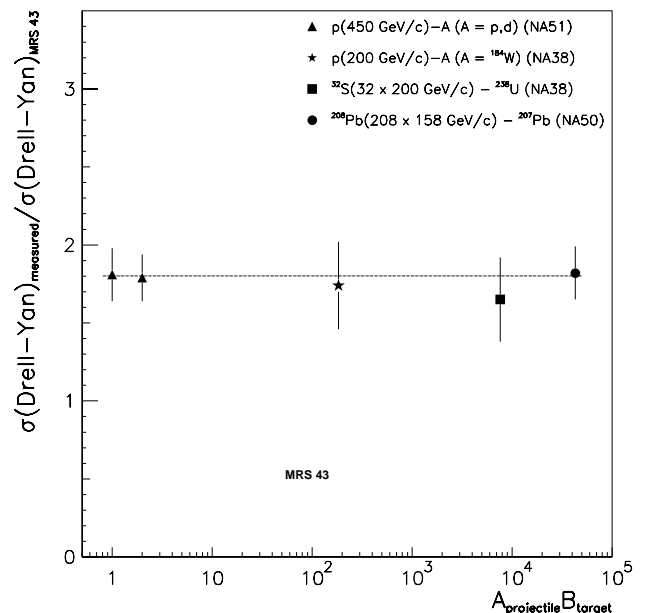


Figure 1: The Drell-Yan cross-section as a function of $A \cdot B$, in terms of the experimental K factor

4 Results

Let us first concentrate on Drell-Yan production. Figure 1 shows for different systems, as a function of the product of projectile and target atomic mass numbers, $A \cdot B$, the measured Drell-Yan cross-section normalized to the theoretical value, computed at the leading order using the MRS43 structure functions. This ratio is the so-called K-factor and is a measure of the higher order corrections needed to account for the data.

The different proton and neutron content of the interacting nuclei are taken into account, by referring all data to p-p collisions, using the relation:

$$\sigma_{DY}^{AB}(corr) = \sigma_{DY}^{AB}(meas) \times \frac{AB \cdot \sigma_{DY}^{pp}(th)}{\sigma_{DY}^{AB}(th)}.$$

All the results are compatible and lead to the average value $K = 1.78 \pm 0.09$, in agreement with expectations.

Using the usual power law behaviour to parametrize the nuclear dependence of hard processes

$$\sigma_{DY}^{AB} = (AB)^\alpha \cdot \sigma_{DY}^{pp},$$

a fit to the data, corrected as explained above, leads to $\alpha = 1.002 \pm 0.011$, in perfect agreement with the expected value $\alpha = 1$.

That is, from p-p up to Pb-Pb the Drell-Yan cross-section behaves normally and is proportional to the number of elementary nucleon-nucleon collisions (i.e., the

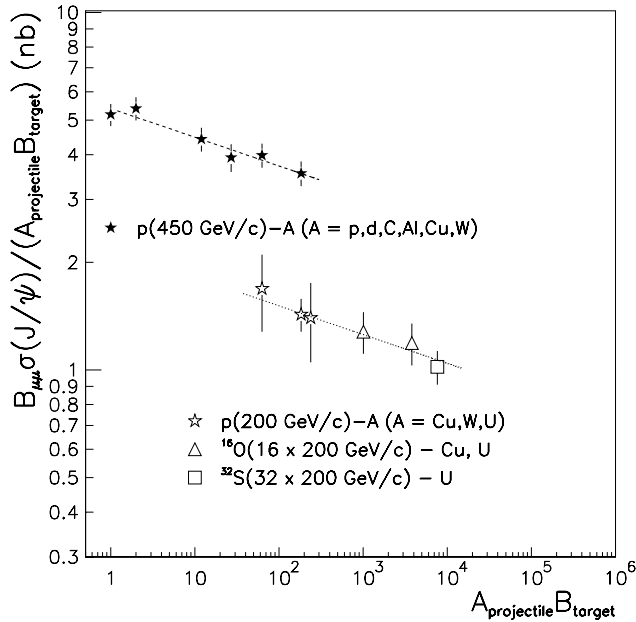


Figure 2: J/ψ cross-section per nucleon-nucleon collision, as a function of $A \cdot B$, for 450 GeV/c and 200 GeV/c incident projectiles, for several systems ranging from p-p to S-U

product $A \cdot B$). Thus, it is useful to use it as a reference to the study of other systems.

In order to compare our new measurements on Pb-Pb with results obtained with proton and other ion induced reactions, and besides the isospin correction discussed above, the measured cross-sections are all rescaled to the same incident beam momentum according to:

$$\sigma_{DY}^{corr}(E_f) = \sigma_{DY}^{meas}(E_i) \times \frac{\sigma_{DY}^{th}(E_f)}{\sigma_{DY}^{th}(E_i)}.$$

We turn now to the study of J/ψ . Figure 2 shows the J/ψ cross-section per nucleon-nucleon collision as a function of $A \cdot B$, for the two data sets, p-A collisions at 450 GeV/c, and proton, oxygen and sulphur induced reactions at 200 GeV/c. The power law behaviour fit gives compatible values, namely $\alpha_{450} = 0.92 \pm 0.02$ and $\alpha_{200} = 0.91 \pm 0.04$. The common trend observed from p-p to S-U allows us to merge all the data on the same curve after energy rescaling (Figure 3). An overall fit leads to $\alpha = 0.92 \pm 0.01$. According to some authors, this behaviour may be interpreted as due to an absorption in nuclear matter of the pre-resonant $c\bar{c}g$ state⁷.

Figure 3 also shows that the Pb-Pb cross-section, rescaled to 200 GeV, lies well below the value expected from the pattern of lighter interacting nuclei. This anomalous suppression can be quantified by the ratio between the measured and expected value, $R_K = 0.74 \pm 0.06$, which includes a 7% systematic error.

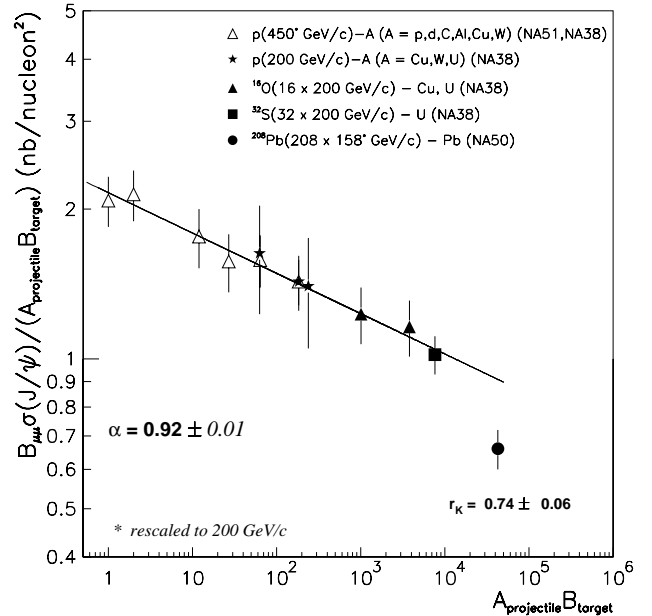


Figure 3: J/ψ cross-section per nucleon-nucleon collision, as a function of $A \cdot B$, for several systems ranging from p-p to Pb-Pb, having rescaled all incident momenta to 200 GeV/c

The J/ψ cross-section per nucleon-nucleon collision can also be estimated from the ratio of the J/ψ to Drell-Yan cross-sections. This ratio is almost free of systematic errors, which are common to both samples (only 1.5% left). In Figure 4 the two samples collected in 1995 and 1996 are shown separately, as a function of E_T . They are significantly different in statistics but are fully compatible with each other. A threshold is clearly seen near 40 GeV in the 1996 sample which, thanks to statistics, can be studied with a much narrower binning.

A common description is needed in order to put together the NA50 data on Pb-Pb with previous NA38 and NA51 data obtained with lighter systems. We define L as the path length of the pre-resonant $c\bar{c}g$ state through nuclear matter. In the framework of a nuclear geometrical model, L can be related to a given impact parameter b . As b and E_T are also related, E_T bins just correspond to different L values. In a given E_T bin, L is computed by averaging the path length over the production point within the nuclei, and the impact parameter.

The J/ψ over Drell-Yan cross-sections' ratio, through its decay into muons, denoted as $B_{\mu\mu}\sigma_{J/\psi}/\sigma_{DY}$, is shown in Figure 5, as a function of L . All 450 GeV/c and 200 GeV/c data have been rescaled to 158 GeV/c using the Schuler parametrization⁶. A good overall fit from p-p to S-U interactions is obtained with an absorption model parametrized as $exp(-\rho L \sigma_{abs})$, where $\rho = 0.17$ nucleons/fm³ is the standard nuclear density. The

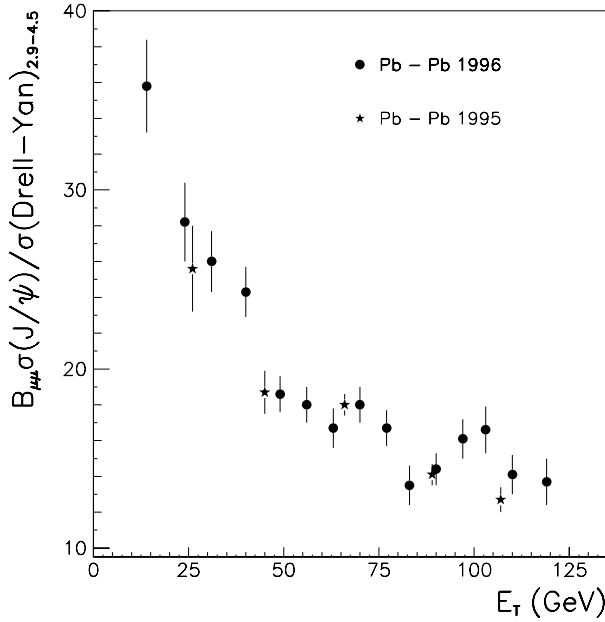


Figure 4: The ratio of J/ψ to Drell-Yan cross-sections as a function of E_T , for two data sets, in Pb-Pb collisions

fit leads to an absorption cross-section $\sigma_{abs} = 5.8 \pm 0.6$ mb, compatible with theoretical predictions⁷. Whereas the more peripheral Pb-Pb points lie on the absorption curve, the more central ones show a clear departure at $L \simeq 8$ fm, suggesting the onset of another J/ψ suppression mechanism. In fact, several authors claim that this behaviour can only be explained in the framework of QGP formation⁸.

Finally, we turn to the study of ψ' production. Because of its larger radius as compared to J/ψ , ψ' should have a lower threshold for breakup. Figure 6 shows as a function of $A \cdot B$, for several systems ranging from p-p to Pb-Pb, the ψ' over J/ψ cross-sections' ratio, $B_{\mu\mu}\sigma_{\psi'}/B_{\mu\mu}\sigma_{J/\psi}$, where $B_{\mu\mu}$ are the branching ratios of J/ψ and ψ' into muons. While ψ' and J/ψ show the same behaviour in proton-nucleus collisions, their ratio has much lower values in ion induced interactions. The ψ' over Drell-Yan ratio, that is, $B_{\mu\mu}\sigma_{\psi'}/\sigma_{DY}$, is plotted in Figure 7 as a function of L , for different proton and ion induced reactions. In proton-nucleus collisions ψ' follows the same nuclear absorption curve as J/ψ , supporting the assumption of a $c\bar{c}g$ state interacting in the target nucleus. But, for S-U and Pb-Pb interactions, ψ' shows an additional suppression, which may be attributed to another mechanism. Several authors have indeed tried to explain it by means of a further ψ' absorption by comovers (hadrons produced in the interaction and accompanying the resonance)⁹. However, this kind of mechanism can hardly account for sudden pattern changes, as

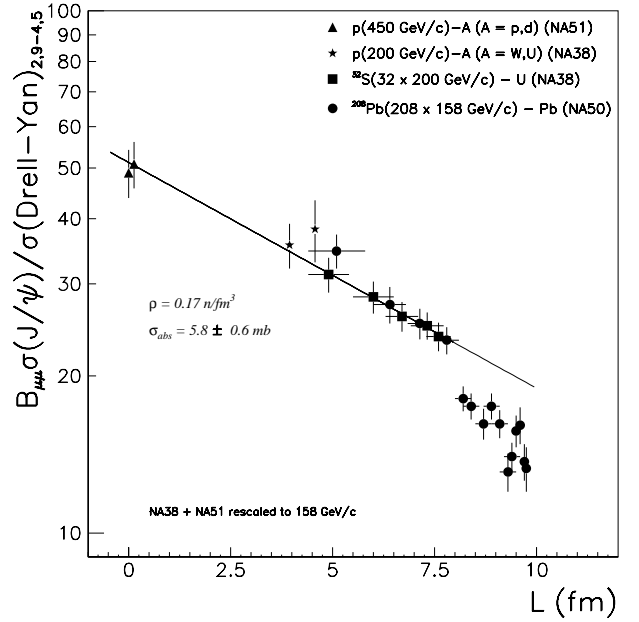


Figure 5: The ratio of J/ψ to Drell-Yan cross-sections as a function of L , for several systems ranging from p-p to Pb-Pb

observed for J/ψ .

5 Conclusions

We have studied the Drell-Yan, J/ψ and ψ' production cross-sections for various systems, ranging from p-p to Pb-Pb interactions. The Drell-Yan production is proportional to the number of collisions, and is thus used as a reference to the study of J/ψ and ψ' . J/ψ follows a nuclear absorption pattern for p-A, S-U, and Pb-Pb peripheral collisions. It shows a clear departure from this absorption trend when centrality increases, exhibiting a sharp decrease at $L \simeq 8$ fm. ψ' behaves, as J/ψ , according to the same absorption curve for proton-nucleus data, but shows a stronger suppression for sulphur and lead induced interactions, which begins at lower L values. This suggests that the suppression mechanism for J/ψ and ψ' are different.

References

1. T. Matsui and H. Satz, *Phys. Lett. B* **178**, 416 (1986).
2. NA50 Collaboration, M.C. Abreu et al., *Phys. Lett. B* **410**, 327 (1997), *Phys. Lett. B* **410**, 337 (1997) and references therein.
3. A.D. Martin et al., *Phys. Lett. B* **306**, 145 (1993).
4. NA51 Collaboration, A. Baldit et al., *Phys. Lett. B* **332**, 244 (1994).

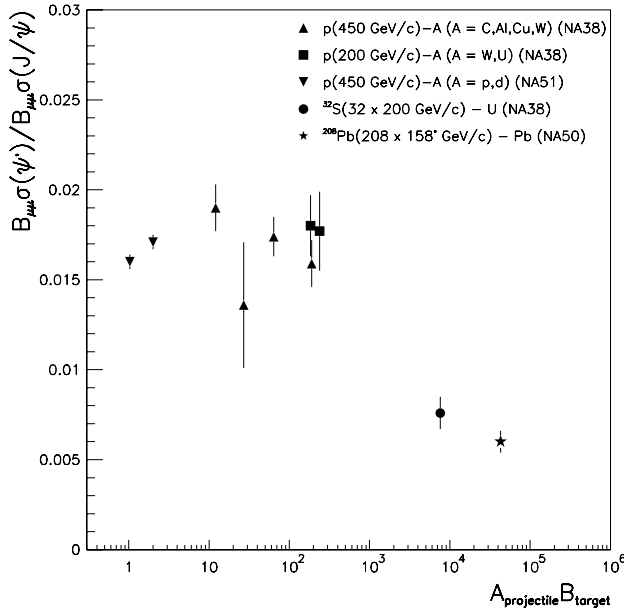


Figure 6: The ratio of ψ' to J/ψ cross-sections as a function of $A \cdot B$, for several systems ranging from p-p to Pb-Pb

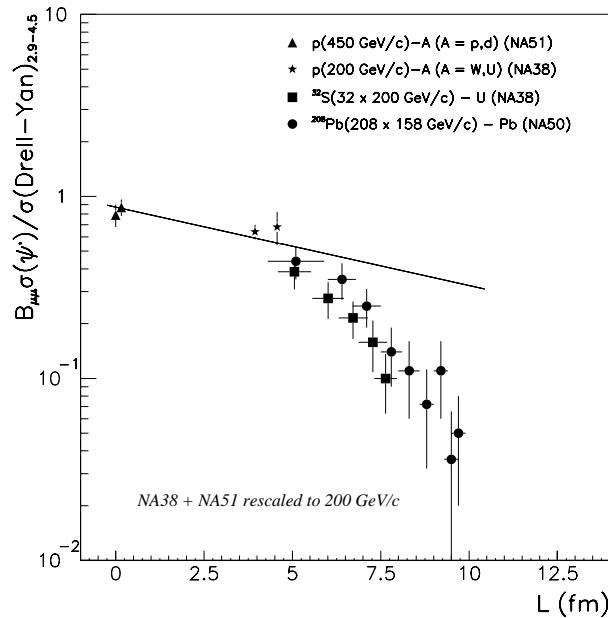


Figure 7: The ratio of ψ' to Drell-Yan cross-sections as a function of L , for several systems ranging from p-p to Pb-Pb

5. See C. Soave's contribution to these Proceedings.
6. G.A. Schuler, CERN-TH 7170/94 (HEP-PH/9403387) (1994).
7. See for instance, D. Kharzeev and H. Satz, *Phys. Lett. B* **366**, 316 (1996).
8. D.Kharzeev, *Nucl. Phys. A* **610**, 418c (1996); C.Y. Wong, *Nucl. Phys. A* **610**, 434c (1996); J.P. Blaizot, J.Y. Ollitrault, *Phys. Rev. Lett.* **77**, 1703 (1996); N. Armesto et al., *Phys. Rev. Lett.* **77**, 3736 (1996); D.Kharzeev et al., *Z. Phys. C* **74**, 307 (1997); M. Nardi and H. Satz, hep-ph/9805247.
9. S. Gavin and R. Vogt, *Phys. Rev. Lett.* **78**, 1006 (1997); A. Capella et al, *Phys. Lett. B* **393**, 431 (1997); W. Cassing and C.M. Ko, *Phys. Lett. B* **396**, 39 (1997).